Two-mode light states before and after delocalized single-photon addition

Bo Lan,[1] Hong-chun Yuan,[2] and Xue-xiang Xu[1,*]

[1]*College of Physics and Communication Electronics, Jiangxi Normal University, Nanchang 330022, China*
[2]*School of Electrical and Information Engineering, Changzhou Institute of Technology, Changzhou 213032, China*

(Received 29 December 2021; revised 7 May 2022; accepted 25 August 2022; published 6 September 2022)

We studied the effect of delocalized single-photon addition (DPA $\hat{a}_1^\dagger + e^{i\varphi}\hat{a}_2^\dagger$) on two input modes containing four cases: two independent coherent states (CSs), two independent thermal states (TSs), two independent single-mode squeezed vacuums (SVs), and an entangled two-mode squeezed vacuum (TMSV). In essence, four types of non-Gaussian entangled light states are generated. We studied three different resources (including entanglement, discorrelation, and Wigner negativity) for each two-mode light state. The output states after DPA are entangled, with more parameters and complex structures, characterizing more Wigner negativity or even discorrelation. In contrast, the CSs case is the most tunable protocol, because its negativity under partial transposition, discorrelation, and Wigner logarithmic negativity are more sensitive to superposition phase φ than those in TSs, SVs, and TMSV cases.

DOI: 10.1103/PhysRevA.106.033703

I. INTRODUCTION

Gaussian entangled states play important roles in continuous-variable (CV) quantum physics [1,2]. As the primary entangled resource, the two-mode squeezed vacuum (TMSV) has been used in many quantum protocols, such as quantum teleportation [3] and quantum computation [4]. However, non-Gaussian states and operations are necessary for many quantum tasks [5]. For example, the NOON state is a useful entangled resource, which has been generated [6] and applied in quantum metrology [7]. The subject of non-Gaussian quantum states has become a very active area of research. A recent tutorial on non-Gaussian states was reported by Walschaers [8]. He provided a roadmap for the physics and an overview of several experimental realizations of non-Gaussian quantum states. Lvovsky *et al.* also reported another review, which covered theoretical and experimental efforts to extend the applications from the Gaussian to the non-Gaussian domain [9]. In essence, non-Gaussian quantum states can be created by applying non-Gaussian operations on the initial states. Moreover, non-Gaussian operations, like single-photon subtraction (by annihilation operator $\hat{a}$) [10] and single-photon addition (by creation operator $a^\dagger$) [11], together with sequence and superpositions of these two operations [12], are essential to exploit quantum resources. These resources (such as entanglement, discorrelation, and Wigner negativity) can provide different quantum advantages in different quantum protocols.

Many efforts have been devoted to classifying and quantifying entanglement for bipartite systems [13,14]. For example, one can measure pure-state entanglement by entropy of entanglement [15] and measure mixed-state entanglement by entanglement of formation [16], entanglement cost [17], relative entropy of entanglement [18], and so on. Vidal and Werner introduced a computable measure of entanglement for the bipartite mixed state. They constructed negativity or a logarithmic negativity base on negativity under partial transposition (NPT) [19]. Later, important developments were made in the optical hybrid approach to quantum information [20,21]. Morin *et al.* proposed and experimentally tested a witness for single-photon entanglement [22]. This witness specially identified entanglement present in the single-photon subspace ($\{|0\rangle, |1\rangle\}$) and used it to witness entanglement for CV quantum states [23–25].

Discorrelation, as a new joint statistical property of multimode quantum light states, was introduced recently by Meyer-Scott *et al.* [26]. Discorrelation is characterized by the fact that the photon number in each mode can take any values, but two modes together never exhibit the same. Indeed, discorrelation can exhibit correlation of photon numbers between different modes. Recently, Biagi *et al.* generated discorrelated states based on delocalized photon addition (DPA) [27,28] and provided experimental observation and application [29]. Indeed, discorrelation can be applied to manipulating the secure distribution of information among untrusted parties, in scenarios such as distributed voting schemes [30] or "mental poker" games [31].

Wigner negativity is an essential resource to reaching a quantum advantage with CVs [32,33]. It has been identified as a necessary ingredient for implementing processes that cannot be simulated efficiently with classical resources [4,34]. Wigner negativity is arguably one of the most striking nonclassical and non-Gaussian features of quantum states. Wigner negativity implies nonclassicality and non-Gaussianity. So far, researchers have proposed many witnesses to quantify Wigner negativity [35–38].

In quantum-state engineering, there is a trend for researchers to prepare multimode [39] or multiphoton non-Gaussian quantum states [40,41]. In the study of states that are both highly non-Gaussian and highly multimode, Walschaers *et al.* even provided a framework which is suited to obtain

*Corresponding author: xuxuexiang@jxnu.edu.cn

general analytical results [42]. Chabaud *et al.* also derived a theoretical framework for the experimental certification of non-Gaussian features of quantum states [43]. Moreover, it has been demonstrated that the entanglement of multimode states can be increased via local or nonlocal operations [44–51]. Indeed, nonlocal operations have the effect of delocalization, which can entangle the input independent states or change the entanglement of the input entangled states.

Then, what is the "delocalized" quantum operation? We consider that if $\hat{O}_j \equiv \hat{O}_j(\hat{a}_j^\dagger, \hat{a}_j)$ denotes the local quantum operation in the jth mode, the coherent superpositions $\sum_{j=1}^n c_j \hat{O}_j$ are referred to as a delocalized quantum operation [where c_j is the superposition coefficient and $\hat{a}_j^\dagger$ ($\hat{a}_j$) is the creation (annihilation) operator]. Undoubtedly, the effect of the coherent superposition $\sum_{j=1}^n c_j \hat{O}_j$ is different from that of the local product $\hat{O}_1\hat{O}_2\cdots\hat{O}_n$. The delocalized quantum operation can change properties of n-mode (independent or entangled) light states and generate new n-mode entangled light states. The possibility of arbitrarily "adding" and "subtracting" single photons to and from a light field may give access to a complete engineering of quantum states [52]. Photon subtraction has been demonstrated as extremely useful for de-Gaussification [53], enhancing nonclassicality [54], and distilling entanglement [55]. Ourjoumtsev *et al.* demonstrated that entanglement can be increased via delocalized single-photon subtraction (DPS $c_1\hat{a}_1 + c_2\hat{a}_2$) [56]. Conversely, photon addition has been demonstrated to create nonclassicality. Recently, Biagi *et al.* presented a scheme to entangle two identical coherent states (CSs) based on the delocalized single-photon addition ($\hat{a}_1^\dagger + e^{i\varphi}\hat{a}_2^\dagger$, where φ denotes the superposition phase) [27–29]. Indeed, all these mode-selective photon additions and subtractions are experimentally promising processes to create multimode non-Gaussian entangled states [57–61].

In this paper, we theoretically study the effect of DPA (i.e., $\hat{a}_1^\dagger + e^{i\varphi}\hat{a}_2^\dagger$) on different input two-mode states. We extend Biagi *et al.*'s work [27] to include additional input states. Therefore, we generate entangled light states and study their entanglement, discorrelation, and Wigner negativity. The remaining paper is organized as follows: In Sec. II, we introduce theoretical schemes and entangled light states. In Sec. III, we witness entanglement for two-mode light states. In Sec. IV, we study their discorrelation. In Sec. V, we study their Wigner negativity. Main results are summarized and discussions are given in Sec. VI.

II. ENTANGLED LIGHT STATES

In 1991, Agarwal and Tara introduced the photon-added coherent state by operating the creation operator on the coherent state [62]. Since then, a lot of similar works (including multimode cases) have been done one after another [63–65]. As depicted schematically in Fig. 1, we consider four types of non-Gaussian entangled light states by employing DPA $\hat{A}_{dl} = \hat{a}_1^\dagger + e^{i\varphi}\hat{a}_2^\dagger$ on different input two-mode states, including two independent CSs, two independent thermal states (TSs), two independent single-mode squeezed vacuums (SVs), and an entangled TMSV.

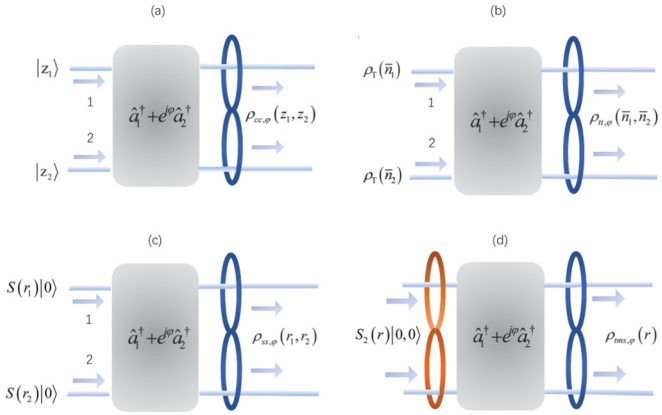

FIG. 1. Conceptual generating schemes of entangled light states $\rho_{\text{out},\varphi}$ by performing DPA $a_1^\dagger + e^{i\varphi}a_2^\dagger$ on different two-mode light states ρ_{in} including (a) two independent CSs, (b) two independent TSs, (c) two independent SVs, and (d) an entangled TMSV.

A. Case CS-CS

The CS in the jth mode is expressed as $|z_j\rangle = e^{-|z_j|^2/2}\sum_{n=0}^\infty \frac{z_j^n}{\sqrt{n!}}|n\rangle$ (where z_j is an arbitrary complex number) [66]. Inputting two independent CSs (i.e., $|z_1\rangle$ and $|z_2\rangle$), the generated state yields

$$|\psi_{cc,\varphi}(z_1,z_2)\rangle_{12} = \frac{1}{\sqrt{N_{cc}}}\hat{A}_{dl}|z_1\rangle|z_2\rangle \tag{1}$$

with normalization factor $N_{cc} = |z_1 + e^{-i\varphi}z_2|^2 + 2$. In this case, the input state is $\rho^{cc}(z_1,z_2) = |z_1\rangle\langle z_1| \otimes |z_2\rangle\langle z_2|$, and the output state is $\rho_{cc,\varphi}(z_1,z_2) = |\psi_{cc,\varphi}(z_1,z_2)\rangle\langle\psi_{cc,\varphi}(z_1,z_2)|$. In particular, when $z_1 = z_2 = \alpha$, the input is reduced to two identical CSs of light in different modes, which is just the case studied in Refs. [27–29]. When $z_1 = 0$ and α, it will degenerate to the case in other literature [67,68].

B. Case TS-TS

The TS in the jth mode is diagonal in the Fock state basis and is expressed as $\rho_T(\bar{n}_j) = \sum_{n_j=0}^\infty P_{n_j}|n_j\rangle\langle n_j|$ [where $P_{n_j} = \bar{n}_j{}^{n_j}/(\bar{n}_j+1)^{n_j+1}$ with mean thermal photon number $\bar{n}_j$]. Inputting two independent TSs [i.e., the input state is $\rho^{tt}(\bar{n}_1,\bar{n}_2) = \rho_T(\bar{n}_1)\otimes\rho_T(\bar{n}_2)$], the output state yields

$$\rho_{tt,\varphi}(\bar{n}_1,\bar{n}_2) = \frac{1}{N_{tt}}\hat{A}_{dl}\rho_T(\bar{n}_1)\rho_T(\bar{n}_2)\hat{A}_{dl}^\dagger \tag{2}$$

with normalization factor $N_{tt} = \bar{n}_1 + \bar{n}_2 + 2$. The TS is the most classical light state and possesses a completely incoherent character. Zavatta and coworkers have realized many light states by manipulating TSs [69,70].

C. Case SV-SV

The SV in the jth mode is expressed as $\hat{S}(r_j)|0\rangle_j = (1-\lambda_j^2)^{1/4}e^{\lambda_j\hat{a}_j^{\dagger 2}/2}|0\rangle_j$ with $\lambda_j = \tanh r_j$ [where $S(r_j) = e^{r_j(\hat{a}_j^{\dagger 2} - \hat{a}_j^2)/2}$ is the single-mode squeezing operator with real r_j] [71]. Inputting two independent SVs [i.e., $\hat{S}(r_1)|0\rangle$ and

$\hat{S}(r_2)|0\rangle$], the generated state yields

$$|\psi_{ss,\varphi}(r_1,r_2)\rangle = \frac{1}{\sqrt{N_{ss}}}\hat{A}_{dl}\hat{S}(r_1)|0\rangle\hat{S}(r_2)|0\rangle \tag{3}$$

with normalization factor $N_{ss} = \kappa_1 + \kappa_2$ [here, $\kappa_j = (1-\lambda_j^2)^{-1}$]. In this case, the input state is $\rho^{ss}(r_1,r_2) = \hat{S}(r_1)|0\rangle\langle 0|\hat{S}^\dagger(r_1) \otimes \hat{S}(r_2)|0\rangle\langle 0|\hat{S}^\dagger(r_2)$ and the output state is $\rho_{ss,\varphi}(r_1,r_2) = |\psi_{ss,\varphi}(r_1,r_2)\rangle\langle\psi_{ss,\varphi}(r_1,r_2)|$.

D. Case TMSV

The TMSV is written by $\hat{S}_2(r)|0_1 0_2\rangle = \sqrt{1-\lambda^2}e^{\lambda\hat{a}_1^\dagger\hat{a}_2^\dagger}|0_1 0_2\rangle$ with $\lambda = \tanh r$ [where $\hat{S}_2(r) = e^{r(\hat{a}_1^\dagger\hat{a}_2^\dagger - \hat{a}_1\hat{a}_2)}$ is the two-mode squeezing operator with real r] [72]. Inputting the TMSV, the generated state yields

$$|\psi_{tms,\varphi}(r)\rangle = \frac{1}{\sqrt{N_{tms}}}\hat{A}_{dl}\hat{S}_2(r)|0_1 0_2\rangle \tag{4}$$

with normalization factor $N_{tms} = 2\kappa$ [here $\kappa = (1-\lambda^2)^{-1}$]. In this case, the input state is $\rho^{tms}(r) = \hat{S}_2(r)|0_1 0_2\rangle\langle 0_1 0_2|\hat{S}_2^\dagger(r)$, and the output state is $\rho_{tms,\varphi}(r) = |\psi_{tms,\varphi}(r)\rangle\langle\psi_{tms,\varphi}(r)|$. Unlike the above three separable cases, the input is an entangled state in itself.

The input-output states in the above schemes can be unified as

$$\rho_{\text{out},\varphi} = \frac{1}{N}\hat{A}_{dl}\rho_{\text{in}}\hat{A}_{dl}^\dagger \tag{5}$$

with normalization factor N. Here ρ_{in}s include $\rho^{cc}(z_1,z_2)$, $\rho^{tt}(\bar{n}_1,\bar{n}_2)$, $\rho^{ss}(r_1,r_2)$, and $\rho^{tms}(r)$ and $\rho_{\text{out},\varphi}$s include $\rho_{cc,\varphi}(z_1,z_2)$, $\rho_{tt,\varphi}(\bar{n}_1,\bar{n}_2)$, $\rho_{ss,\varphi}(r_1,r_2)$, and $\rho_{tms,\varphi}(r)$. Density operators are provided in Appendix A and normalization factors are derived in Appendix B. In order to compare, we often simulate properties by using the same $\bar{n}_{T,\text{in}}$ (input total mean photon number), that is, $|z_1|^2 + |z_2|^2 = \bar{n}_{T,\text{in}}$, $\bar{n}_1 + \bar{n}_2 = \bar{n}_{T,\text{in}}$, $\sinh^2 r_1 + \sinh^2 r_2 = \bar{n}_{T,\text{in}}$, and $2\sinh^2 r = \bar{n}_{T,\text{in}}$. When inputting $|0\rangle_1|0\rangle_2$, the output will be a single-photon mode-entangled state $|\psi_{00}\rangle = \frac{1}{\sqrt{2}}(|1\rangle_1|0\rangle_2 + e^{i\varphi}|0\rangle_1|1\rangle_2)$ [67]. Once we let $z_1 = z_2 = 0$, $\bar{n}_1 = \bar{n}_2 = 0$, $r_1 = r_2 = 0$, or $r = 0$, states in Eqs. (1)–(4) are reduced to $\rho_{00} = |\psi_{00}\rangle\langle\psi_{00}|$.

In what follows, we shall analyze entanglement, discorrelation, and Wigner negativity for all these two-mode light states.

III. ENTANGLEMENT OF TWO-MODE LIGHT STATES

In this section, we shall quantify their entanglement by NPT [13,14,19,73], a witness proposed by Morin *et al.* [22]. The remarkable feature of this witness lies in dimension independence for the measured state. Here, we make a brief review of NPT.

First, we project measured state ρ into subspace $\{|00\rangle, |01\rangle, |10\rangle$ and $|11\rangle\}$ and obtain a 4×4 matrix with form

$$X = \frac{1}{T}\begin{pmatrix} p_{00,00} & p_{00,01} & p_{00,10} & p_{00,11} \\ p_{01,00} & p_{01,01} & p_{01,10} & p_{01,11} \\ p_{10,00} & p_{10,01} & p_{10,10} & p_{10,11} \\ p_{11,00} & p_{11,01} & p_{11,10} & p_{11,11} \end{pmatrix}, \tag{6}$$

where $p_{k_1k_2,l_1l_2} = \langle k_1,k_2|\rho|l_1,l_2\rangle$ and $T = p_{00,00} + p_{01,01} + p_{10,10} + p_{11,11}$ (ensuring $\text{Tr}X = 1$) [22–25]. Thus, the full density matrix was restricted to such subspace. Here, X is Hermitian and has non-negative eigenvalues, the trace norm of which holds $\|X\|_1 \equiv \text{Tr}(\sqrt{X^\dagger X}) = \text{Tr}X = 1$ [19].

Second, performing partial transposition in mode 2 for X, we obtain a matrix with form

$$X^{T_2} = \frac{1}{T}\begin{pmatrix} p_{00,00} & p_{01,00} & p_{00,10} & p_{01,10} \\ p_{00,01} & p_{01,01} & p_{00,11} & p_{01,11} \\ p_{10,00} & p_{11,00} & p_{10,10} & p_{11,10} \\ p_{10,01} & p_{11,01} & p_{10,11} & p_{11,11} \end{pmatrix}, \tag{7}$$

with $X^{T_2}_{k_1l_2,l_1,k_2} = X_{k_1k_2,l_1,l_2} = \langle k_1,k_2|X|l_1,l_2\rangle$, and further calculate eigenvalues of X^{T_2}. Certainly, X^{T_2} also satisfies $\text{Tr}X^{T_2} = 1$. In general, the trace norm of X^{T_2} reads $\|X^{T_2}\|_1 \equiv 1 - 2\sum_i \lambda_i^-$, where λ_i^- denotes negative eigenvalues of X^{T_2} [19].

Lastly, we quantify entanglement by NPT defined as

$$\text{NPT}(\rho) = -2\sum_i \lambda_i^-, \tag{8}$$

where the factor of -2 ensures $0 \leqslant \text{NPT}(\rho) \leqslant 1$ [43–45].

Indeed, NPT measures entanglement by considering how much X^{T_2} fails to be positive definite. If X^{T_2} has at least one negative eigenvalue, ρ is inseparable (or entangled). NPT is zero for a completely separable state (the X^{T_2} of which has no negative eigenvalues) and 1 for a maximally entangled one [74].

One can resort to $p_{k_1k_2,l_1,l_2} = \langle k_1,k_2|\rho|l_1,l_2\rangle$ in Appendix C and eigenvalues of X^{T_2}s in Appendix D to obtain NPTs.

(1) NPT of $\rho_{cc,\varphi}$ is calculated as

$$\text{NPT}[\rho_{cc,\varphi}(z_1,z_2)] = \frac{2}{|z_1 + e^{-i\varphi}z_2|^2 + 2}. \tag{9}$$

This result can be reduced to $\text{NPT}[\rho_{cc,\varphi}(z,z)] = 1/[1 + |z|^2(1+\cos\varphi)]$ [27].

(2) NPT of $\rho_{tt,\varphi}$ is calculated as

$$\text{NPT}[\rho_{tt,\varphi}(\bar{n}_1,\bar{n}_2)] = \frac{\sqrt{4A^2+\Gamma^2} - \Gamma}{2A+\Gamma}, \tag{10}$$

with $A = (1+\bar{n}_1)(1+\bar{n}_2)$ and $\Gamma = \bar{n}_1 + \bar{n}_2 + 2\bar{n}_1\bar{n}_2$. Note that $\text{NPT}(\rho_{tt,\varphi})$ is independent of φ.

(3) NPT of $\rho_{ss,\varphi}$ is calculated as

$$\text{NPT}[\rho_{ss,\varphi}(r_1,r_2)] = 1. \tag{11}$$

This means that $\rho_{ss,\varphi}$ keeps maximum entanglement independently of r_1, r_2, and φ.

(4) NPT of $\rho_{tms,\varphi}$ is calculated as

$$\text{NPT}[\rho_{tms,\varphi}(r)] = 1. \tag{12}$$

This means that $\rho_{tms,\varphi}$ keeps maximum entanglement independently of r and φ.

In Fig. 2, we plot NPTs for $\rho_{cc,\varphi}$ in (z_1,z_2) space with different φ $(0,\pi/2,\pi)$ and for $\rho_{tt,\varphi}$ in $(\bar{n}_1,\bar{n}_2)$ space with arbitrary φ. Without loss of generality, z_1 and z_2 take real numbers. It is noteworthy that $\text{NPT}(\rho_{cc,\varphi})$ can reach 1 at $z_1 = z_2 = 0$ for any φ [see Figs. 2(a) and 2(b)] and $\text{NPT}[\rho_{cc,\pi}(z,z)] = 1$ is always satisfied [see Fig. 2(c)]. From Fig. 2(d), we see

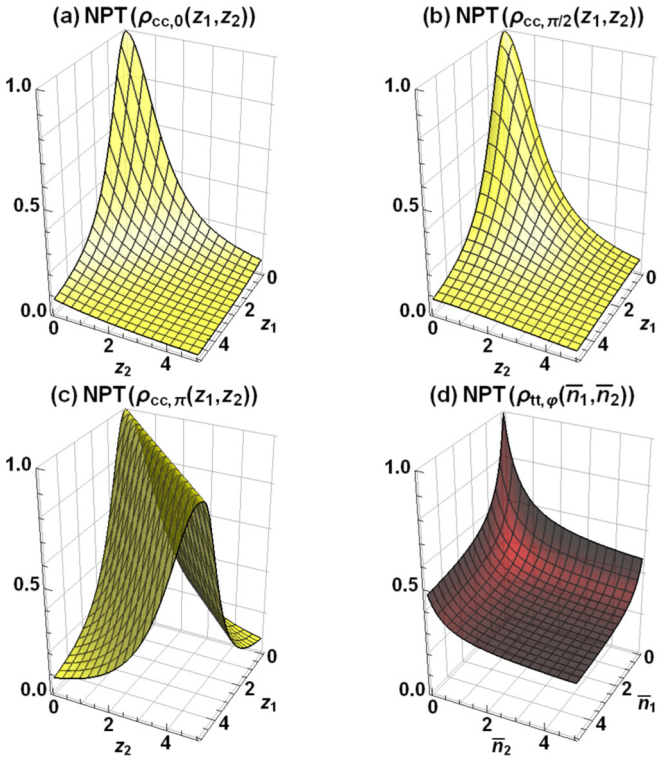

FIG. 2. Plots of NPTs for (a) $\rho_{cc,0}$, (b) $\rho_{cc,\pi/2}$, and (c) $\rho_{cc,\pi}$ in (z_1, z_2) space and (d) $\rho_{tt,\varphi}$ in $(\bar{n}_1, \bar{n}_2)$ space.

that NPT($\rho_{tt,\varphi}$) reaches 1 at $\bar{n}_1 = \bar{n}_2 = 0$ and decreases as $\bar{n}_1$ (or $\bar{n}_2$) increases. But NPTs of $\rho_{ss,\varphi}$ and $\rho_{tms,\varphi}$ are always 1 independent of parameters. All cases can be reduced to NPT(ρ_{00}) = 1 as expected.

In Fig. 3, we plot several NPTs as functions of $\bar{n}_{T,\text{in}}$. We find that NPT$[\rho_{cc,\pi}(z,z)]$, NPT$[\rho_{ss,\varphi}(r_1,r_2)]$, and NPT$[\rho_{tms,\varphi}(r)]$ are always 1, showing their robust entanglements. These states maintain constant maximum entanglement independently of parameters, while NPT$[\rho_{cc,\varphi}(z,z)]$s except $\varphi = \pi$ are monotone decreasing functions of $\bar{n}_{T,\text{in}}$. For a given $\bar{n}_{T,\text{in}}$, the larger φ is, the larger NPT$[\rho_{cc,\varphi}(z,z)]$ is. Of course, NPT$[\rho_{tt,\varphi}(\bar{n},\bar{n})]$ is also a monotonically decreasing function of $\bar{n}_{T,\text{in}}$, which is independent of φ.

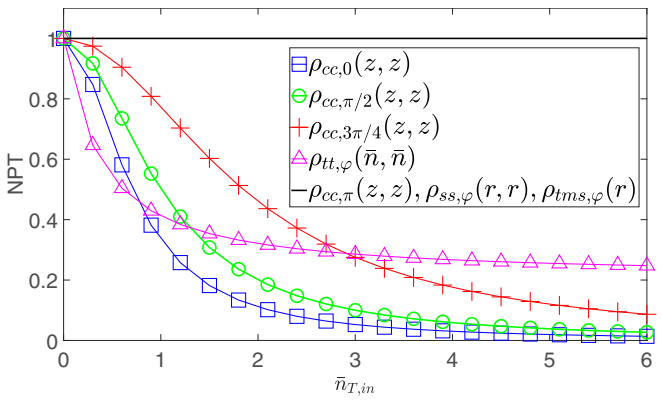

FIG. 3. NPTs as functions of $\bar{n}_{T,\text{in}}$ for different $\rho_{\text{out},\varphi}$s.

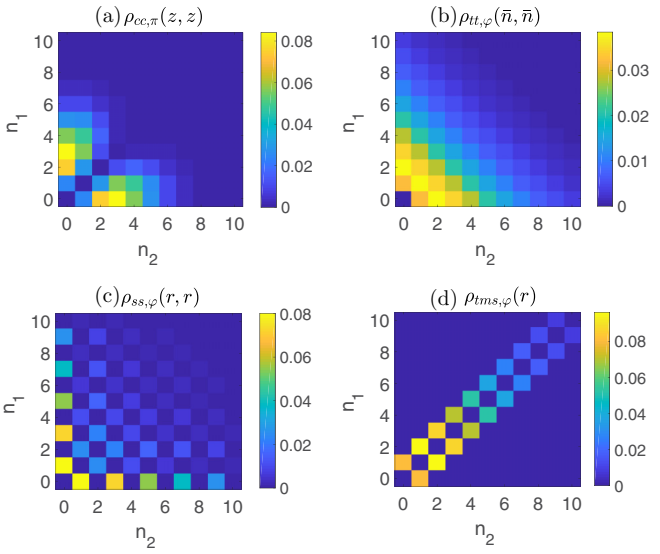

FIG. 4. JPNDs of states (a) $\rho_{cc,\pi}(z,z)$, (b) $\rho_{tt,\varphi}(\bar{n},\bar{n})$, (c) $\rho_{ss,\varphi}(r,r)$, and (d) $\rho_{tms,\varphi}(r)$, with $\bar{n}_{T,\text{in}} = 3$.

IV. DISCORRELATION OF TWO-MODE LIGHT STATES

Discorrelation is used to show correlation of joint photon number distributions (JPNDs). For two-mode light states, the JPND is defined by $P_{n_1,n_2} = \langle n_1, n_2|\rho|n_1, n_2\rangle$ (where n_j denotes the photon number in mode j). If $P_{n,n} \equiv 0$ for all n, but $P_{n_1,\cdot} = \sum_{n_2=0}^{\infty} P_{n_1,n_2}$ and $P_{\cdot,n_2} = \sum_{n_1=0}^{\infty} P_{n_1,n_2}$ are nonzero, then this two-mode state is a discorrelated state [26–29]. All JPNDs can be calculated from $p_{k_1k_2,l_1l_2} = \langle k_1, k_2|\rho|l_1, l_2\rangle$ in Appendix C.

JPNDs for $\rho_{cc,\pi}(z,z)$, $\rho_{tt,\varphi}(\bar{n},\bar{n})$, $\rho_{ss,\varphi}(r,r)$, and $\rho_{tms,\varphi}(r)$ with $\bar{n}_{T,\text{in}} = 3$ are plotted in Fig. 4. From Fig. 4(a), we can affirm that only $\rho_{cc,\pi}(z,z)$ is a discorrelated state because $P_{n,n} = 0$ may hold only if $z_1 = z_2$ and $\varphi = \pi$. From Fig. 4(b), we can affirm that $\rho_{tt,\varphi}(\bar{n}_1,\bar{n}_2)$ is not a discorrelated state except $\bar{n}_1 = \bar{n}_2 = 0$. As $\bar{n}_1$ and $\bar{n}_2$ increase, JPNDs of $\rho_{tt,\varphi}$ cannot meet characteristics of discorrelation. From Fig. 4(c), we can affirm that $\rho_{ss,\varphi}(r_1,r_2)$ is a discorrelated state because $P_{n,n} \equiv 0$ is always right regardless of r_1, r_2, and φ. From Fig. 4(d), we can affirm that $\rho_{tms,\varphi}(r)$ is a discorrelated state,

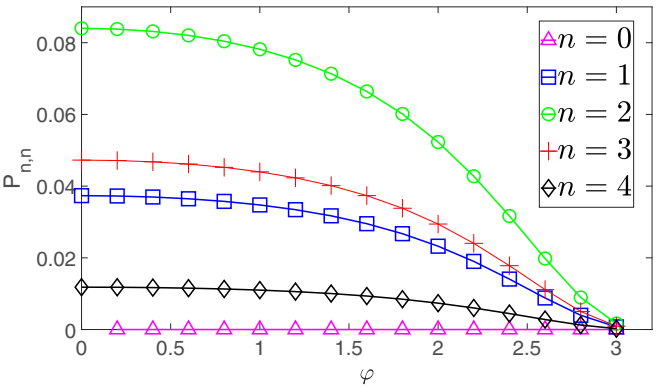

FIG. 5. $P_{n,n}$s as functions of phase φ for $\rho_{cc,\varphi}(\sqrt{1.5}, \sqrt{1.5})$, with $P_{n,n} \equiv 0$ at $\varphi = \pi$.

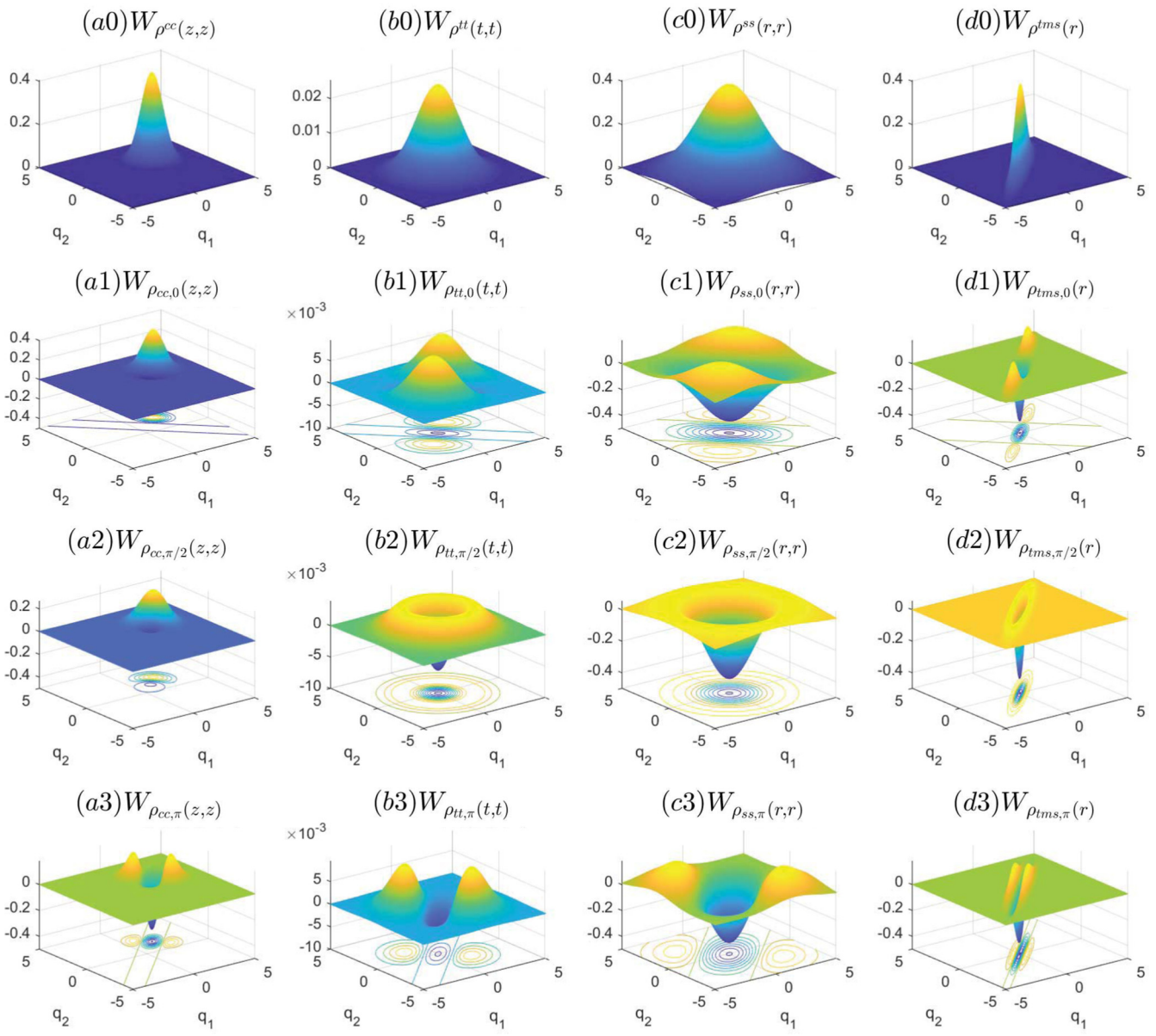

FIG. 6. Plots of $W_\rho(q_1, 0; q_2, 0)$ in (q_1, q_2) space for (a) ρ^{cc} and $\rho_{cc,\varphi}$ with $\varphi = 0, \pi/2, \pi$; (b) ρ^{tt} and $\rho_{tt,\varphi}$ with $\varphi = 0, \pi/2, \pi$; (c) ρ^{ss} and $\rho_{ss,\varphi}$ with $\varphi = 0, \pi/2, \pi$; and (d) ρ^{tms} and $\rho_{tms,\varphi}$ with $\varphi = 0, \pi/2, \pi$. Here, their inputs are symmetrical with $\bar{n}_{T,\text{in}} = 3$.

which also can be analyzed from twin-Fock distribution of TMSV [75]. Of course, ρ_{00} is a special discorrelated state.

Figure 5 presents $P_{n,n}$s (with $n = 0, 1, 2, 3, 4$) as functions of phase φ for $\rho_{cc,\varphi}(\sqrt{1.5}, \sqrt{1.5})$. As φ increases in interval $[0, \pi]$, each $P_{n,n}$ (except $n = 0$) decreases monotonically. Until $\varphi = \pi$, we always have $P_{n,n} = 0$, which is a necessary condition of discorrelation. However, $\rho_{cc,\varphi}$s with $\varphi \neq \pi$ are not discorrelated states because $P_{n,n} = 0$ is not always satisfied for any nonzero z_1, z_2.

V. WIGNER NEGATIVITY OF TWO-MODE LIGHT STATES

The Wigner function (WF) can exhibit negative values for some non-Gaussian states. Wigner negativity, as a nonclassical indicator [36,76–78] with non-Gaussian character [37,38,79], plays an essential role in quantum computing and simulation [4,80]. Of course, Wigner negativity can be detected [81] or demonstrated [82] in current technology.

The WF of a two-mode light state ρ can be calculated as $W_\rho(\beta_1, \beta_2) = \langle \Pi(\beta_1)\Pi(\beta_2)\rangle_\rho$. Here, $\Pi(\beta_j) = \frac{2}{\pi} D(\beta_j)(-1)^{\hat{a}_j^\dagger \hat{a}_j} D^\dagger(\beta_j)$ and $D(\beta_j) = e^{\beta_j \hat{a}_j^\dagger - \beta_j \hat{a}_j}$ denote the Wigner operator and displacement operator for mode j, respectively, with $\beta_j = (q_j + ip_j)/\sqrt{2}$. Obviously, $W_\rho(\beta_1, \beta_2)$ is real and bounded by $-4/\pi^2 \leqslant W_\rho(\beta_1, \beta_2) \leqslant 4/\pi^2$.

Interestingly, W_{ρ_in} and $W_{\rho_{\text{out},\varphi}}$ can be linked by

$$W_{\rho_{\text{out},\varphi}}(\beta_1, \beta_2) = \frac{T^{\text{NG}}}{N} W_{\rho_\text{in}}(\beta_1, \beta_2), \tag{13}$$

where T^{NG} and N denote the non-Gaussian term and normalization factor, respectively. All analytical expressions can be obtained from Appendix E. The results show that all W_{ρ_in}s

are Gaussian and all $W_{\rho_{\text{out},\varphi}}$s are non-Gaussian. If condition $T^{\text{NG}} < 0$ is satisfied, the negativity of $W_{\rho_{\text{out},\varphi}}$ is exhibited.

A. Case CS-CS

We can obtain $W_{\rho_{cc,\varphi}}$ after knowing

$$W_{\rho^{cc}} = \frac{4e^{-2|z_1-\beta_1|^2-2|z_2-\beta_2|^2}}{\pi^2}, \tag{14}$$

and

$$T_{cc}^{\text{NG}} = |(z_1 - 2\beta_1) + e^{-i\varphi}(z_2 - 2\beta_2)|^2 - 2. \tag{15}$$

B. Case TS-TS

We can obtain $W_{\rho_{tt,\varphi}}$ after knowing

$$W_{\rho^{tt}} = \frac{4e^{-\frac{2}{2\bar{n}_1+1}|\beta_1|^2-\frac{2}{2\bar{n}_2+1}|\beta_2|^2}}{\pi^2(2\bar{n}_1+1)(2\bar{n}_2+1)} \tag{16}$$

and

$$T_{tt}^{\text{NG}} = 4|\epsilon_1\beta_1 + e^{-i\varphi}\epsilon_2\beta_2|^2 - (\epsilon_1 + \epsilon_2) \tag{17}$$

with $\epsilon_j = (\bar{n}_j + 1)/(2\bar{n}_j + 1)$.

C. Case SV-SV

We can obtain $W_{\rho_{ss,\varphi}}$ after knowing

$$W_{\rho^{ss}} = \frac{4e^{-2\kappa_1|\lambda_1\beta_1-\beta_1^*|^2-2\kappa_2|\lambda_2\beta_2-\beta_2^*|^2}}{\pi^2} \tag{18}$$

and

$$T_{ss}^{\text{NG}} = 4|\kappa_1(\lambda_1\beta_1 - \beta_1^*) + e^{-i\varphi}\kappa_2(\lambda_2\beta_2 - \beta_2^*)|^2 - (\kappa_1 + \kappa_2). \tag{19}$$

D. Case TMSV

We can obtain $W_{\rho_{tms,\varphi}}$ after knowing

$$W_{\rho^{tms}} = \frac{4}{\pi^2}e^{-2\kappa(|\lambda\beta_1-\beta_2^*|^2+|\lambda\beta_2-\beta_1^*|^2)} \tag{20}$$

and

$$T_{tms}^{\text{NG}} = 4\kappa^2|(\lambda\beta_1 - \beta_2^*) + e^{-i\varphi}(\lambda\beta_2 - \beta_1^*)|^2 - 2\kappa. \tag{21}$$

Using the above expressions, we can obtain $W_{\rho_{\text{out},\varphi}}$ for each case, which can be reduced to the following extreme case:

$$W_{\rho_{00}} = \frac{4(2|\beta_1 + e^{-i\varphi}\beta_2|^2 - 1)}{\pi^2}e^{-2(|\beta_1|^2+|\beta_2|^2)}. \tag{22}$$

The distribution $W_\rho(\beta_1, \beta_2)$ can be expressed in the four-dimensional phase space as $W_\rho(q_1, p_1; q_2, p_2)$, which shows correlations existing in four quadratures $(\hat{q}_1,\ \hat{p}_1,\ \hat{q}_2,\ \hat{p}_2)$. Here, $\hat{q}_j = (\hat{a}_j + \hat{a}_j^\dagger)/\sqrt{2}$ and $\hat{p}_j = (\hat{a}_j - \hat{a}_j^\dagger)/(i\sqrt{2})$ denote the position operator and momentum operator of mode j, respectively. $W_{\rho_{00}}(\beta_1, \beta_2)$ was pictorially demonstrated by Ourjoumtsev *et al.* [56]. Figure 6 presents contour plots of $W_\rho(q_1, 0; q_2, 0)$ in the $(q_1,\ q_2)$ section for each case with one-input ρ_{in} and three-output $\rho_{\text{out},\varphi}$ $(\varphi = 0, \pi/2, \pi)$. Before DPA, the input WFs are Gaussian without Wigner negativity. But after DPA, the output WFs will be non-Gaussian with Wigner negativity.

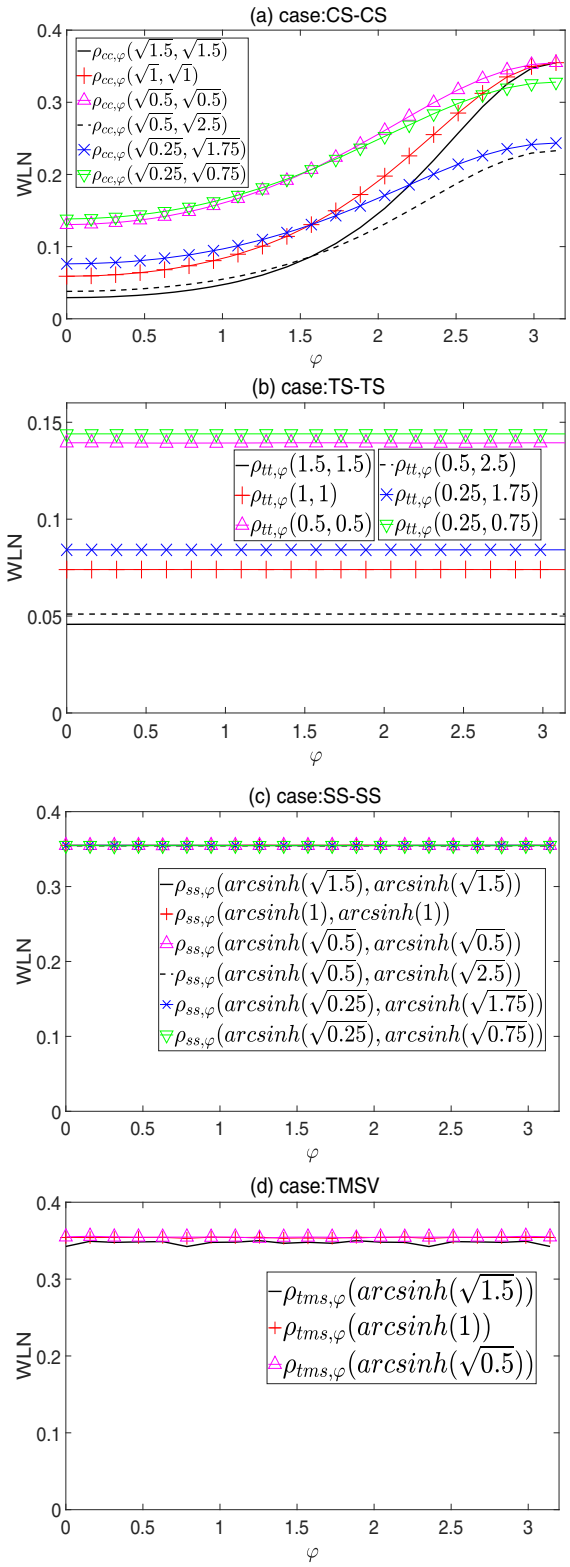

FIG. 7. WLNs as functions of φ for states (a) $\rho_{cc,\varphi}(z_1, z_2)$ with different z_1 and z_2, where the maximal WLN values at $\varphi = \pi$ are corresponding to 0.35, 0.328, 0.244, and 0.233 from top to bottom; (b) $\rho_{tt,\varphi}(\bar{n}_1, \bar{n}_2)$ with different $(\bar{n}_1, \bar{n}_2)$, where the WLN values are corresponding to 0.144, 0.139, 0.084, 0.074, 0.051, and 0.046 from top to bottom; (c) $\rho_{ss,\varphi}(r_1, r_2)$ with different r_1 and r_2, where the WLN values are equal to 0.35; and (d) $\rho_{tms,\varphi}(r)$ with different r, where the WLN values are equal to or slightly smaller than 0.35.

TABLE I. Results of NPT and entanglement for all two-mode light states considered in this paper.

	NPT	Entangled or separable
$\rho^{cc}(z_1, z_2)$	0	Separable
$\rho_{cc,\varphi}(z_1, z_2)$	$\frac{2}{\lvert z_1+e^{-i\varphi}z_2\rvert^2+2}$	Entangled
$\rho^{tt}(\bar{n}_1, \bar{n}_2)$	0	Separable
$\rho_{tt,\varphi}(\bar{n}_1, \bar{n}_2)$	$\frac{\sqrt{4A^2+\Gamma^2}-\Gamma}{2A+\Gamma}$	Entangled
$\rho^{ss}(r_1, r_2)$	0	Separable
$\rho_{ss,\varphi}(r_1, r_2)$	1	Entangled
$\rho^{tms}(r)$	$\frac{2\lambda}{1+\lambda^2}$	Entangled
$\rho_{tms,\varphi}(r)$	1	Entangled

From a quantitative perspective, we can measure Wigner negativity by quantifying Wigner logarithmic negativity (WLN) [37,38]. Here, the WLN is defined by

$$\mathrm{WLN} = \ln\left[\int |W_\rho(\beta_1, \beta_2)| d^2\beta_1 d^2\beta_2\right], \tag{23}$$

which shows non-Gaussianity of the quantum state. By fixing $\bar{n}_{T,\mathrm{in}} = 1$, 2, and 3, we plot WLN behaviors as functions of φ in the interval $[0, \pi]$ for different $\rho_{\mathrm{out},\varphi}$s in Fig. 7. The results show the following.

(1) WLNs of $\rho_{cc,\varphi}$s are monotone increasing functions of φ. For symmetrical $z_1 = z_2$ cases, the maximum WLNs are equal to 0.35 at $\varphi = \pi$, while for asymmetrical $z_1 \neq z_2$ cases, the maximum WLNs are smaller than 0.35 at $\varphi = \pi$.

(2) WLNs of $\rho_{tt,\varphi}$s are independent of φ but determined by $\bar{n}_1$ and $\bar{n}_2$. The larger $\bar{n}_{T,\mathrm{in}}$ is, the smaller WLN is. As $\bar{n}_{T,\mathrm{in}}$ increases, the WLNs limit to zero. Moreover, WLN for the asymmetrical case is bigger than that for the symmetrical case for fixing $\bar{n}_{T,\mathrm{in}}$.

(3) WLNs of $\rho_{ss,\varphi}(r)$ will remain at 0.35 for any r_1, r_2, and φ.

(4) WLNs of $\rho_{ss,\varphi}(r)$ will be about 0.35 for any r and φ. Indeed WLN of ρ_{00} is always 0.35 for any φ.

VI. CONCLUSION AND DISCUSSION

In summary, we have studied NPT, discorrelation, and WLN for four different two-mode states subjected to a DPA operator. The four two-mode states are two independent CSs, two independent TSs, two independent SVs, and a TMSV, which are the common quantum states in the field of quantum optics. We calculated that all four of these states lead to non-Gaussian entangled states following DPA. Based on NPTs, we concluded entanglement in Table I. Based on proper criteria, we concluded discorrelation in Table II. We also calculated WLNs to exhibit Wigner negativity. In contrast, we still think that the CSs protocol is the most tunable. This is because NPT, discorrelation, and WLN in the CSs case are all very sensitive to φ and reach maximal values (or effects) at $\varphi = \pi$. So $\rho_{cc,\varphi}$s have good controllability by adjusting φ, while, in TSs, SVs, and TMSV protocols, NPT, discorrelation, and WLN are independent of φ. Moreover, SVs and TMSV after DPA do not exhibit more entanglement and Wigner negativity than $|0\rangle_1|0\rangle_2$ after DPA, which can be seen from their NPTs and WLNs. Worst of all, as thermal photon number increases, TSs after DPA have lower NPT and WLN than $|0\rangle_1|0\rangle_2$ after DPA, with discorrelation disappearance.

TABLE II. Results of discorrelation for all two-mode light states considered in this paper.

	Discorrelation	Conditions
$\rho^{cc}(z_1, z_2)$	No	For arbitrary z_1 and z_2
$\rho_{cc,\varphi}(z_1, z_2)$	Yes	Only if $z_1 = z_2$ and $\varphi = \pi$
$\rho^{tt}(\bar{n}_1, \bar{n}_2)$	No	For arbitrary $\bar{n}_1$ and $\bar{n}_2$
$\rho_{tt,\varphi}(\bar{n}_1, \bar{n}_2)$	No	For nonzero $\bar{n}_1$, $\bar{n}_2$, and φ
$\rho^{ss}(r_1, r_2)$	No	For arbitrary r_1 and r_2
$\rho_{ss,\varphi}(r_1, r_2)$	Yes	For arbitrary r_1, r_2, and φ
$\rho^{tms}(r)$	No	For arbitrary r
$\rho_{tms,\varphi}(r)$	Yes	For arbitrary r and φ

We regret that our schemes are ideal without considering decoherence (including losses or detection efficiency). Recently, Walschaers *et al.* used the framework of open quantum systems and master equations to describe losses in all modes of the considered protocol [83]. This provided us a reference for our future works. Rather than changing input states, we can also generalize $\hat{a}_1^\dagger + e^{i\varphi}\hat{a}_2^\dagger$ to multiphoton cases, such as $\hat{a}_1^{\dagger m_1} + e^{i\varphi}\hat{a}_2^{\dagger m_2}$ or $(\hat{a}_1^\dagger + e^{i\varphi}\hat{a}_2^\dagger)^m$. Broadly, $\hat{a}_1^\dagger + e^{i\varphi}\hat{a}_2^\dagger$ can be extended to $c_1\hat{O}_1(\hat{a}_1^\dagger, \hat{a}_1) + c_2\hat{O}_2(\hat{a}_2^\dagger, \hat{a}_2)$, including $\hat{a}_1 + e^{i\varphi}\hat{a}_2$. In addition, we can extend from two-mode to multimode cases.

So far, in relation to applications or quantum technologies, many breakthroughs of delocalized photon addition or subtraction were reported. Roeland *et al.* developed a general framework for mode-selective single-photon addition to a multimode quantum field [84]. Barral and Linares proposed a versatile integrated optical chip and generated both nonlocal addition and subtraction on SVs [85]. Barral *et al.* produced a reconfigurable superposition of photon subtraction on two SVs [86]. Nehra *et al.* produced a variety of non-Gaussian states by using coherent photon subtraction from a TMSV [87]. So, we also anticipate that our considered states will be generated in state-of-the-art quantum optics experiments and will be used as resources in quantum technologies.

ACKNOWLEDGMENTS

This paper was supported by the National Natural Science Foundation of China (Grant No. 11665013). We would like to thank Qiongyi He, Yu Xiang, Shengli Zhang, Bixuan Fan, and Zhenglu Duan for useful discussions.

APPENDIX A: UNIFYING EXPRESSIONS OF DENSITY OPERATORS

Obviously, once we assume

$$\rho_{h_1,h_2,t_1,t_2} = \hat{a}_1^{\dagger h_1}\hat{a}_2^{\dagger h_2}\rho_{\mathrm{in}}\hat{a}_1^{t_1}\hat{a}_2^{t_2} \tag{A1}$$

(here, h_1, h_2, t_1, and t_2 are non-negative integers), we can obtain ρ_{in} by using $\rho_{\mathrm{in}} = \rho_{0,0,0,0}$ and $\rho_{\mathrm{out},\varphi}$ by using

$$\rho_{\mathrm{out},\varphi} = N^{-1}(\rho_{1,0,1,0} + \rho_{0,1,0,1} + e^{-i\varphi}\rho_{1,0,0,1} + e^{i\varphi}\rho_{0,1,1,0}). \tag{A2}$$

In the following calculation, we rewrite ρ_{h_1,h_2,t_1,t_2} as

$$\rho_{h_1,h_2,t_1,t_2} = \partial_{\mu_1}^{h_1}\partial_{\mu_2}^{h_2}\partial_{\nu_1}^{t_1}\partial_{\nu_2}^{t_2} e^{\mu_1\hat{a}_1^\dagger} e^{\mu_2\hat{a}_2^\dagger}\rho_{\rm in} e^{\nu_1\hat{a}_1} e^{\nu_2\hat{a}_2}|_{\mu_1=\mu_2=\nu_1=\nu_2=0}, \tag{A3}$$

where $a_j^{\dagger h_j} = \partial_{\mu_j}^{h_j} e^{\mu_j\hat{a}_j^\dagger}|_{\mu_j=0}$ and $a_j^{t_j} = \partial_{\nu_j}^{t_j} e^{\nu_j\hat{a}_j}|_{\nu_j=0}$ have been used.

APPENDIX B: NORMALIZATION FACTORS OF $\rho_{\rm out,\varphi}$

As long as we know $\mathrm{Tr}\rho_{h_1,h_2,t_1,t_2}$, we can obtain normalization factor N for $\rho_{\rm out,\varphi}$ by

$$N = \mathrm{Tr}\rho_{1,0,1,0} + \mathrm{Tr}\rho_{0,1,0,1} + e^{-i\varphi}\mathrm{Tr}\rho_{1,0,0,1} + e^{i\varphi}\mathrm{Tr}\rho_{0,1,1,0}. \tag{B1}$$

Next we give $\mathrm{Tr}\rho_{h_1,h_2,t_1,t_2}$ for each case.

(I) For case CS-CS, we have

$$\mathrm{Tr}\rho^{cc}_{h_1,h_2,t_1,t_2} = \partial_{\mu_1}^{h_1}\partial_{\mu_2}^{h_2}\partial_{\nu_1}^{t_1}\partial_{\nu_2}^{t_2} e^{\mu_1\nu_1+\nu_1 z_1+\mu_1 z_1^*} e^{\mu_2\nu_2+\nu_2 z_2+\mu_2 z_2^*}|_{\mu_1=\mu_2=\nu_1=\nu_2=0}, \tag{B2}$$

which determines $\mathrm{Tr}\rho^{cc}_{1,0,1,0} = |z_1|^2+1$, $\mathrm{Tr}\rho^{cc}_{0,1,0,1} = |z_2|^2+1$, $\mathrm{Tr}\rho^{cc}_{1,0,0,1} = z_1^* z_2$, $\mathrm{Tr}\rho^{cc}_{0,1,1,0} = z_1 z_2^*$, and $N_{cc} = |z_1 + e^{-i\varphi}z_2|^2 + 2$.

(II) For case TS-TS, we have

$$\mathrm{Tr}\rho^{tt}_{h_1,h_2,t_1,t_2} = \partial_{\mu_1}^{h_1}\partial_{\mu_2}^{h_2}\partial_{\nu_1}^{t_1}\partial_{\nu_2}^{t_2} e^{(\bar{n}_1+1)\mu_1\nu_1} e^{(\bar{n}_2+1)\mu_2\nu_2}|_{\mu_1=\mu_2=\nu_1=\nu_2=0}, \tag{B3}$$

which determines $\mathrm{Tr}\rho^{tt}_{1,0,1,0} = \bar{n}_1+1$, $\mathrm{Tr}\rho^{tt}_{0,1,0,1} = \bar{n}_2+1$, $\mathrm{Tr}\rho^{tt}_{1,0,0,1} = 0$, $\mathrm{Tr}\rho^{tt}_{0,1,1,0} = 0$, and $N_{tt} = \bar{n}_1+\bar{n}_2+2$.

(III) For case SV-SV, we have

$$\mathrm{Tr}\rho^{ss}_{h_1,h_2,t_1,t_2} = \partial_{\mu_1}^{h_1}\partial_{\mu_2}^{h_2}\partial_{\nu_1}^{t_1}\partial_{\nu_2}^{t_2} e^{\kappa_1\mu_1\nu_1+\lambda_1\kappa_1(\nu_1^2+\mu_1^2)/2} e^{\kappa_2\mu_2\nu_2+\lambda_2\kappa_2(\nu_2^2+\mu_2^2)/2}|_{\mu_1=\mu_2=\nu_1=\nu_2=0}, \tag{B4}$$

which determines $\mathrm{Tr}\rho^{ss}_{1,0,1,0} = \kappa_1$, $\mathrm{Tr}\rho^{ss}_{0,1,0,1} = \kappa_2$, $\mathrm{Tr}\rho^{ss}_{1,0,0,1} = 0$, $\mathrm{Tr}\rho^{ss}_{0,1,1,0} = 0$, and $N_{ss} = \kappa_1+\kappa_2$.

(IV) For case TMSV, we have

$$\mathrm{Tr}\rho^{tms}_{h_1,h_2,t_1,t_2} = \partial_{\mu_1}^{h_1}\partial_{\mu_2}^{h_2}\partial_{\nu_1}^{t_1}\partial_{\nu_2}^{t_2} e^{\kappa(\mu_1\nu_1+\mu_2\nu_2)} e^{\lambda\kappa(\mu_1\mu_2+\nu_1\nu_2)}|_{\mu_1=\mu_2=\nu_1=\nu_2=0}, \tag{B5}$$

which determines $\mathrm{Tr}\rho^{tms}_{1,0,1,0} = \mathrm{Tr}\rho^{tms}_{0,1,0,1} = \kappa$, $\mathrm{Tr}\rho^{12}_{1,0,0,1} = \mathrm{Tr}\rho^{12}_{0,1,1,0} = 0$, and $N_{tms} = 2\kappa$.

APPENDIX C: DENSITY-MATRIX ELEMENTS IN FOCK BASIS

If we know

$$p_{h_1,h_2,t_1,t_2,k_1k_2,l_1l_2} = \langle k_1|\langle k_2|\rho_{h_1,h_2,t_1,t_2}|l_1\rangle|l_2\rangle, \tag{C1}$$

we can easily obtain $p^{\rm in}_{k_1k_2,l_1l_2} = p_{0,0,0,0,k_1k_2,l_1l_2}$ for $\rho_{\rm in}$ and

$$p^{\rm out}_{k_1k_2,l_1l_2} = N^{-1}(p_{1,0,1,0,k_1k_2,l_1l_2} + p_{0,1,0,1,k_1k_2,l_1l_2} + e^{-i\varphi}p_{1,0,0,1,k_1k_2,l_1l_2} + e^{i\varphi}p_{0,1,1,0,k_1k_2,l_1l_2}) \tag{C2}$$

for $\rho_{\rm out,\varphi}$. By employing $\langle k_j| = \frac{1}{\sqrt{k_j!}}\partial_{m_j}^{k_j}\langle 0|e^{m_j\hat{a}_j}|_{m_j=0}$ and $|l_j\rangle = \frac{1}{\sqrt{l_j!}}\partial_{n_j}^{l_j} e^{n_j\hat{a}_j^\dagger}|0\rangle|_{n_j=0}$, we have

$$\begin{aligned} p_{h_1,h_2,t_1,t_2,k_1k_2,l_1l_2} = {} & \frac{1}{\sqrt{k_1!k_2!l_1!l_2!}}\partial_{m_1}^{k_1}\partial_{m_2}^{k_2}\partial_{n_1}^{l_1}\partial_{n_2}^{l_2}\partial_{\mu_1}^{h_1}\partial_{\mu_2}^{h_2}\partial_{\nu_1}^{t_1}\partial_{\nu_2}^{t_2}\langle 0|_1\langle 0|_2 e^{m_1\hat{a}_1} e^{m_2\hat{a}_2} e^{\mu_1\hat{a}_1^\dagger} e^{\mu_2\hat{a}_2^\dagger}\rho_{\rm in} e^{\nu_1\hat{a}_1} e^{\nu_2\hat{a}_2} \\ & \times e^{n_1\hat{a}_1^\dagger} e^{n_2\hat{a}_2^\dagger}|0\rangle_1|0\rangle_2|_{\mu_1=\mu_2=\nu_1=\nu_2=m_1=m_2=n_1=n_2=0}. \end{aligned} \tag{C3}$$

(I) For case CS-CS, we have

$$\begin{aligned} p^{cc}_{h_1,h_2,t_1,t_2,k_1k_2,l_1l_2} = {} & \frac{1}{\sqrt{k_1!l_1!k_2!l_2!}}\partial_{m_1}^{k_1}\partial_{m_2}^{k_2}\partial_{n_1}^{l_1}\partial_{n_2}^{l_2}\partial_{\mu_1}^{h_1}\partial_{\mu_2}^{h_2}\partial_{\nu_1}^{t_1}\partial_{\nu_2}^{t_2} \\ & \times e^{-|z_1|^2+m_1(\mu_1+z_1)+n_1(\nu_1+z_1^*)-|z_2|^2+m_2(\mu_2+z_2)+n_2(\nu_2+z_2^*)}|_{m_1=\mu_1=\nu_1=n_1=m_2=\mu_2=\nu_2=n_2=0}. \end{aligned} \tag{C4}$$

(II) For case TS-TS, we have

$$p^{tt}_{h_1,h_2,t_1,t_2,k_1,k_2,l_1,l_2} = \frac{A^{-1}}{\sqrt{k_1!l_1!k_2!l_2!}}\partial_{m_1}^{k_1}\partial_{m_2}^{k_2}\partial_{n_1}^{l_1}\partial_{n_2}^{l_2}\partial_{\mu_1}^{h_1}\partial_{\mu_2}^{h_2}\partial_{\nu_1}^{t_1}\partial_{\nu_2}^{t_2} e^{m_1\mu_1+m_2\mu_2+\nu_1 n_1+\nu_2 n_2+\frac{\bar{n}_1}{\bar{n}_1+1}m_1 n_1+\frac{\bar{n}_2}{\bar{n}_2+1}m_2 n_2}|_{m_1=\mu_1=\nu_1=n_1=m_2=\mu_2=\nu_2=n_2=0}. \tag{C5}$$

(III) For case SV-SV, we have

$$p^{ss}_{h_1,h_2,t_1,t_2,k_1k_2,l_1l_2} = \frac{(\kappa_1\kappa_2)^{-1/2}}{\sqrt{k_1!l_1!k_2!l_2!}}\partial_{m_1}^{k_1}\partial_{m_2}^{k_2}\partial_{n_1}^{l_1}\partial_{n_2}^{l_2}\partial_{\mu_1}^{h_1}\partial_{\mu_2}^{h_2}\partial_{\nu_1}^{t_1}\partial_{\nu_2}^{t_2} e^{m_1\mu_1+\frac{\lambda_1}{2}m_1^2+\nu_1 n_1+\frac{\lambda_1}{2}n_1^2+m_2\mu_2+\frac{\lambda_2}{2}m_2^2+\nu_2 n_2+\frac{\lambda_2}{2}n_2^2}|_{\mu_1=\mu_2=\nu_1=\nu_2=m_1=m_2=n_1=n_2=0}. \tag{C6}$$

(IV) For case TMSV, we have

$$p^{tms}_{h_1,h_2,t_1,t_2,k_1k_2,l_1l_2} = \frac{\kappa^{-1}}{\sqrt{k_1!k_2!l_1!l_2!}}\partial^{k_1}_{m_1}\partial^{k_2}_{m_2}\partial^{l_1}_{n_1}\partial^{l_2}_{n_2}\partial^{h_1}_{\mu_1}\partial^{h_2}_{\mu_2}\partial^{t_1}_{\nu_1}\partial^{t_2}_{\nu_2}e^{m_1\mu_1+m_2\mu_2+n_1\nu_1+n_2\nu_2+\lambda m_1m_2+\lambda n_1n_2}|_{m_1=m_2=\mu_1=\mu_2=\upsilon_1=\nu_2=n_1=n_2=0}. \quad \text{(C7)}$$

APPENDIX D: X^{T_2} OF THESE STATES AND THEIR EIGENVALUES

Using p_{k_1,k_2,l_1,l_2} in Appendix C, we obtain X^{T_2}s and calculate their eigenvalues.

(I) Case CS-CS: For $\rho^{cc}(z_1, z_2)$, we obtain matrix

$$X^{T_2}_{\rho^{cc}(z_1,z_2)} = \frac{1}{M}\begin{pmatrix} 1 & z_2 & z_1^* & z_2z_1^* \\ z_2^* & |z_2|^2 & z_1^*z_2^* & |z_2|^2z_1^* \\ z_1 & z_1z_2 & |z_1|^2 & z_2|z_1|^2 \\ z_1z_2^* & z_1|z_2|^2 & z_2^*|z_1|^2 & |z_1|^2|z_2|^2 \end{pmatrix} \quad \text{(D1)}$$

with $M = (1 + |z_1|^2)(1 + |z_2|^2)$, the eigenvalues of which include 1, 0, 0, and 0. Obviously, there is no negative eigenvalue. For $\rho_{cc,\varphi}(z_1, z_2)$, we obtain matrix

$$X^{T_2}_{\rho_{cc,\varphi}(z_1,z_2)} = \begin{pmatrix} 0 & 0 & 0 & \frac{e^{-i\varphi}}{N_{cc}} \\ 0 & \frac{1}{N_{cc}} & 0 & \frac{z_1+e^{-i\varphi}z_2}{N_{cc}} \\ 0 & 0 & \frac{1}{N_{cc}} & \frac{e^{-i\varphi}z_1^*+z_2^*}{N_{cc}} \\ \frac{e^{i\varphi}}{N_{cc}} & \frac{z_1^*+e^{i\varphi}z_2^*}{N_{cc}} & \frac{e^{i\varphi}z_1+z_2}{N_{cc}} & \frac{|z_1+e^{-i\varphi}z_2|^2}{N_{cc}} \end{pmatrix} \quad \text{(D2)}$$

with $N_{cc} = 2 + |z_1 + e^{-i\varphi}z_2|^2$, the eigenvalues of which include $-N_{cc}^{-1}$, N_{cc}^{-1}, $\frac{1}{2}(1 - \sqrt{1 - 4N_{cc}^{-2}})$, and $\frac{1}{2}(1 - \sqrt{1 + 4N_{cc}^{-2}})$. It has a negative eigenvalue $-N_{cc}^{-1}$.

(II) Case TS-TS: For $\rho^{tt}(\overline{n}_1, \overline{n}_2)$, we obtain matrix

$$X^{T_2}_{\rho^{tt}(\overline{n}_1,\overline{n}_2)} = \begin{pmatrix} \frac{A}{B} & 0 & 0 & 0 \\ 0 & \frac{(1+\overline{n}_1)\overline{n}_2}{B} & 0 & 0 \\ 0 & 0 & \frac{\overline{n}_1(1+\overline{n}_2)}{B} & 0 \\ 0 & 0 & 0 & \frac{\overline{n}_1\overline{n}_2}{B} \end{pmatrix} \quad \text{(D3)}$$

with $A = (1 + \overline{n}_1)(1 + \overline{n}_2)$ and $B = (1 + 2\overline{n}_1)(1 + 2\overline{n}_2)$, the eigenvalues of which include $\overline{n}_1\overline{n}_2B^{-1}$, AB^{-1}, $\overline{n}_1(1 + \overline{n}_2)B^{-1}$, and $(1 + \overline{n}_1)\overline{n}_2B^{-1}$. Clearly, there was no negative eigenvalue. For $\rho_{tt,\varphi}(\overline{n}_1, \overline{n}_2)$, we obtain matrix

$$X^{T_2}_{\rho_{tt,\varphi}(\overline{n}_1,\overline{n}_2)} = \begin{pmatrix} 0 & 0 & 0 & \frac{Ae^{i\varphi}}{2A+\Gamma} \\ 0 & \frac{A}{2A+\Gamma} & 0 & 0 \\ 0 & 0 & \frac{A}{2A+\Gamma} & 0 \\ \frac{Ae^{-i\varphi}}{2A+\Gamma} & 0 & 0 & \frac{\Gamma}{2A+\Gamma} \end{pmatrix}, \quad \text{(D4)}$$

the eigenvalues of which include $A/(2A + \Gamma)$, $A/(2A + \Gamma)$, $-\frac{1}{2}(\sqrt{4A^2 + \Gamma^2} - \Gamma)/(2A + \Gamma)$, and $\frac{1}{2}(\sqrt{4A^2 + \Gamma^2} + \Gamma)/(2A + \Gamma)$ with $\Gamma = \overline{n}_1 + \overline{n}_2 + 2\overline{n}_1\overline{n}_2$. It has a negative eigenvalue.

(III) Case SV-SV: For $\rho^{ss}(r_1, r_2)$, we obtain matrix

$$X^{T_2}_{\rho^{ss}(r_1,r_2)} = \begin{pmatrix} 1 & 0 & 0 & 0 \\ 0 & 0 & 0 & 0 \\ 0 & 0 & 0 & 0 \\ 0 & 0 & 0 & 0 \end{pmatrix}, \quad \text{(D5)}$$

the eigenvalues of which include 1, 0, 0, and 0. Obviously, there is no negative eigenvalue. For $\rho_{ss,\varphi}(r_1, r_2)$, we obtain matrix

$$X^{T_2}_{\rho_{ss,\varphi}(r_1,r_2)} = \begin{pmatrix} 0 & 0 & 0 & \frac{e^{i\varphi}}{2} \\ 0 & \frac{1}{2} & 0 & 0 \\ 0 & 0 & \frac{1}{2} & 0 \\ \frac{e^{-i\varphi}}{2} & 0 & 0 & 0 \end{pmatrix}, \quad \text{(D6)}$$

the eigenvalues of which include $-\frac{1}{2}$, $\frac{1}{2}$, $\frac{1}{2}$, and $\frac{1}{2}$. It has one negative eigenvalue $-\frac{1}{2}$.

(IV) Case TMSV: For $\rho^{tms}(r)$, we obtain matrix

$$X^{T_2}_{\rho^{tms}(r)} = \begin{pmatrix} \frac{1}{1+\lambda^2} & 0 & 0 & 0 \\ 0 & 0 & \frac{\lambda}{1+\lambda^2} & 0 \\ 0 & \frac{\lambda}{1+\lambda^2} & 0 & 0 \\ 0 & 0 & 0 & \frac{\lambda^2}{1+\lambda^2} \end{pmatrix} \quad \text{(D7)}$$

the eigenvalues of which include $\frac{1}{\lambda^2+1}$, $-\frac{\lambda}{\lambda^2+1}$, $\frac{\lambda^2}{\lambda^2+1}$, and $\frac{\lambda}{\lambda^2+1}$. Obviously, there is one negative eigenvalue $-\frac{\lambda}{\lambda^2+1}$. For $\rho_{ss,\varphi}(r_1, r_2)$, we obtain matrix

$$X^{T_2}_{\rho_{tms,\varphi}(r)} = \begin{pmatrix} 0 & 0 & 0 & \frac{e^{i\varphi}}{2} \\ 0 & \frac{1}{2} & 0 & 0 \\ 0 & 0 & \frac{1}{2} & 0 \\ \frac{e^{-i\varphi}}{2} & 0 & 0 & 0 \end{pmatrix}, \quad \text{(D8)}$$

the eigenvalues of which include $-\frac{1}{2}$, $\frac{1}{2}$, $\frac{1}{2}$, and $\frac{1}{2}$. It has one negative eigenvalue $-\frac{1}{2}$.

APPENDIX E: WIGNER FUNCTIONS OF THESE STATES

In normal ordering form, we have $\Pi(\beta_j) = \frac{2}{\pi} : e^{-2(\hat{a}_j^\dagger - \beta_j^*)(\hat{a}_j - \beta_j)} :$ ($: \cdots :$ denotes normal ordering). As long as we know $W_{\rho_{h_1,h_2,t_1,t_2}}(\beta_1, \beta_2)$, we can obtain $W_{\rho_{\rm in}}(\beta_1, \beta_2) = W_{\rho_{0,0,0,0}}(\beta_1, \beta_2)$ and

$$\begin{aligned} &W_{\rho_{{\rm out},\varphi}}(\beta_1, \beta_2) \\ &\quad = N^{-1}[W_{\rho_{1,0,1,0}}(\beta_1, \beta_2) + W_{\rho_{0,1,0,1}}(\beta_1, \beta_2) \\ &\qquad + e^{-i\varphi}W_{\rho_{1,0,0,1}}(\beta_1, \beta_2) + e^{i\varphi}W_{\rho_{0,1,1,0}}(\beta_1, \beta_2)]. \end{aligned} \quad \text{(E1)}$$

Next we give $W_{\rho_{h_1,h_2,t_1,t_2}}(\beta_1, \beta_2)$ for each case.

(I) For case CS-CS, we have

$$W_{\rho^{cc}_{h_1,h_2,t_1,t_2}}(\beta_1,\beta_2) = W_{\rho^{cc}(z_1,z_2)}(\beta_1,\beta_2)\partial_{\mu_1}^{h_1}\partial_{\mu_2}^{h_2}\partial_{\nu_1}^{t_1}\partial_{\nu_2}^{t_2} e^{(2\beta_1^*-z_1^*)\mu_1+(2\beta_1-z_1)\nu_1-\mu_1\nu_1} \times e^{(2\beta_2^*-z_2^*)\mu_2+(2\beta_2-z_2)\nu_2-\mu_2\nu_2}|_{\mu_1=\mu_2=\nu_1=\nu_2=0}. \tag{E2}$$

(II) For case TS-TS, we have

$$W_{\rho^{tt}_{h_1,h_2,t_1,t_2}}(\beta_1,\beta_2) = W_{\rho^{tt}(\bar{n}_1,\bar{n}_2)}(\beta_1,\beta_2)\partial_{\mu_1}^{h_1}\partial_{\mu_2}^{h_2}\partial_{\nu_1}^{t_1}\partial_{\nu_2}^{t_2} \times e^{\epsilon_1(2\beta_1^*\mu_1+2\beta_1\nu_1-\mu_1\nu_1)+\epsilon_2(2\beta_2^*\mu_2+2\beta_2\nu_2-\mu_2\nu_2)}|_{\mu_1=\mu_2=\nu_1=\nu_2=0}. \tag{E3}$$

(III) For case SV-SV, we have

$$W_{\rho^{ss}_{h_1,h_2,t_1,t_2}}(\beta_1,\beta_2) = W_{\rho^{ss}(r_1,r_2)}(\beta_1,\beta_2)\partial_{\mu_1}^{h_1}\partial_{\mu_2}^{h_2}\partial_{\nu_1}^{t_1}\partial_{\nu_2}^{t_2} e^{\kappa_1(2\beta_1^*\mu_1+2\beta_1\nu_1-\nu_1\mu_1)+\kappa_2(2\beta_2^*\mu_2+2\beta_2\nu_2-\nu_2\mu_2)} \times e^{\lambda_1\kappa_1(+\frac{1}{2}\nu_1^2+\frac{1}{2}\mu_1^2-2\nu_1\beta_1^*-2\beta_1\mu_1)} e^{\lambda_2\kappa_2(+\frac{1}{2}\nu_2^2+\frac{1}{2}\mu_2^2-2\nu_2\beta_2^*-2\beta_2\mu_2)}|_{\mu_1=\mu_2=\nu_1=\nu_2=0}. \tag{E4}$$

(IV) For case TMSV, we have

$$W_{\rho^{tms}_{h_1,h_2,t_1,t_2}}(\beta_1,\beta_2) = W_{\rho^{tms}(r)}(\beta_1,\beta_2)\partial_{\mu_1}^{h_1}\partial_{\mu_2}^{h_2}\partial_{\nu_1}^{t_1}\partial_{\nu_2}^{t_2} e^{\kappa(2\beta_1^*\mu_1+2\beta_1\nu_1+2\beta_2^*\mu_2+2\beta_2\nu_2-\nu_1\mu_1-\nu_2\mu_2)} \times e^{\lambda\kappa(\nu_1\nu_2+\mu_1\mu_2-2\beta_1\mu_2-2\beta_1^*\nu_2-2\beta_2^*\nu_1-2\beta_2\mu_1)}|_{\mu_1=\mu_2=\nu_1=\nu_2=0}. \tag{E5}$$

[1] S. L. Braunstein and P. van Loock, Quantum information with continuous variables, Rev. Mod. Phys. **77**, 513 (2005).

[2] C. Weedbrook, S. Pirandola, R. Garcia-Patron, N. J. Cerf, T. C. Ralph, J. H. Shapiro, and S. Lloyd, Gaussian quantum information, Rev. Mod. Phys. **84**, 621 (2012).

[3] S. L. Braunstein and H. J. Kimble, Teleportation of Continuous Quantum Variables, Phys. Rev. Lett. **80**, 869 (1998).

[4] A. Mari and J. Eisert, Positive Wigner Functions Render Classical Simulation of Quantum Computation Efficient, Phys. Rev. Lett. **109**, 230503 (2012).

[5] Q. T. Zhuang, P. W. Shor, and J. H. Shapiro, Resource theory of non-Gaussian operations, Phys. Rev. A **97**, 052317 (2018).

[6] Y. A. Chen, X. H. Bao, Z. S. Yuan, S. Chen, B. Zhao, and J. W. Pan, Heralded Generation of an Atomic NOON State, Phys. Rev. Lett. **104**, 043601 (2010).

[7] J. P. Dowling, Quantum optical metrology-the lowdown on high-N00N states, Contemp. Phys. **49**, 125 (2008).

[8] M. Walschaers, Non-Gaussian quantum states and where to find them, PRX Quantum **2**, 030204 (2021).

[9] A. I. Lvovsky, P. Grangier, A. Ourjoumtsev, V. Parigi, M. Sasaki, and R. Tualle-Brouri, Production and applications of non-Gaussian quantum states of light, arXiv:2006.16985 (2020).

[10] A. Ourjoumtsev, R. Tualle-Brouri, J. Laurat, and P. Grangier, Generating optical Schrödinger kittens for quantum information processing, Science **312**, 83 (2006).

[11] A. Zavatta, S. Viciani, and M. Bellini, Quantum-to-classical transition with single-photon-added coherent states of light, Science **306**, 660 (2004).

[12] M. S. Kim, H. Jeong, A. Zavatta, V. Parigi, and M. Bellini, Scheme for Proving the Bosonic Commutation Relation Using Single-Photon Interference, Phys. Rev. Lett. **101**, 260401 (2008).

[13] A. Peres, Separability Criterion for Density Matrices, Phys. Rev. Lett. **77**, 1413 (1996).

[14] M. Horodecki, P. Horodecki, and R. Horodecki, Separability of mixed states: Necessary and sufficient conditions, Phys. Lett. A **223**, 1 (1996).

[15] C. H. Bennett, H. J. Bernstein, S. Popescu, and B. Schumacher, Concentrating partial entanglement by local operations, Phys. Rev. A **53**, 2046 (1996).

[16] C. H. Bennett, D. P. DiVincenzo, J. A. Smolin, and W. K. Wootters, Mixed-state entanglement and quantum error correction, Phys. Rev. A **54**, 3824 (1996).

[17] P. M. Hayden, M. Horodecki, and B. M. Terhal, The asymptotic entanglement cost of preparing a quantum state, J. Phys. A: Math. Gen. **34**, 6891 (2001).

[18] V. Vedral and M. B. Plenio, Entanglement measures and purification procedures, Phys. Rev. A **57**, 1619 (1998).

[19] G. Vidal and R. F. Werner, Computable measure of entanglement, Phys. Rev. A **65**, 032314 (2002).

[20] P. van Loock, Optical hybrid approaches to quantum information, Laser Photonics Rev. **5**, 167 (2011).

[21] H. Jeong, A. Zavatta, M. Kang, S. Lee, L. S. Costanzo, S. Grandi, T. C. Ralph, and M. Bellini, Generation of hybrid entanglement of light, Nat. Photonics **8**, 564 (2014).

[22] O. Morin, J. D. Bancal, M. Ho, P. Sekatski, V. D'Auria, N. Gisin, J. Laurat, and N. Sangouard, Witnessing Trustworthy Single-Photon Entanglement with Local Homodyne Measurements, Phys. Rev. Lett. **110**, 130401 (2013).

[23] C. W. Chou, H. de Riedmatten, D. Felinto, S. V. Polyakov, S. J. van Enk, and H. J. Kimble, Measurement-induced entanglement for excitation stored in remote atomic ensembles, Nature (London) **438**, 828 (2005).

[24] J. Laurat, K. S. Choi, H. Deng, C. W. Chou, and H. J. Kimble, Heralded Entanglement between Atomic Ensembles: Preparation, Decoherence, and Scaling, Phys. Rev. Lett. **99**, 180504 (2007).

[25] M. Ho, O. Morin, J. D. Bancal, N. Gisin, N. Sangouard, and J. Laurat, Witnessing single-photon entanglement with local homodyne measurements: Analytical bounds and robustness to losses, New J. Phys. **16**, 103035 (2014).

[26] E. Meyer-Scott, J. Tiedau, G. Harder, L. K. Shalm, and T. J. Bartley, Discorrelated quantum states, Sci. Rep. **7**, 41622 (2017).

[27] N. Biagi, L. S. Costanzo, M. Bellini, and A. Zavatta, Entangling Macroscopic Light States by Delocalized Photon Addition, Phys. Rev. Lett. **124**, 033604 (2020).

[28] N. Biagi, S. Francesconi, A. Zavatta, and M. Bellini, Coherent superpositions of photon creation operations and their application to multimode states of light, Entropy **23**, 999 (2021).

[29] N. Biagi, L. S. Costanzo, M. Bellini, and A. Zavatta, Generating discorrelated states for quantum information protocols by coherent multimode photon addition, Adv. Quantum Technol. **4**, 2000141 (2021).

[30] J. M. Bohli, J. Müller-Quade, and S. Röhrich, in *E-Voting and Identity*, edited by A. Alkassar and M. Volkamer (Springer-Verlag, Berlin, Heidelberg, 2007), pp. 111–124.

[31] A. Shamir, R. L. Rivest, and L. M. Adleman, *The Mathematical Gardner* (Springer, New York, 1981).

[32] M. Walschaers and N. Treps, Remote Generation of Wigner Negativity through Einstein-Podolsky-Rosen Steering, Phys. Rev. Lett. **124**, 150501 (2020).

[33] Y. Xiang, S. H. Liu, J. J. Guo, Q. H. Gong, N. Treps, Q. Y. He, and M. Walschaers, Distribution and quantification of remotely generated Wigner negativity, npj Quantum Inf. **8**, 21 (2022).

[34] S. Rahimi-Keshari, T. C. Ralph, and C. M. Caves, Sufficient Conditions for Efficient Classical Simulation of Quantum Optics, Phys. Rev. X **6**, 021039 (2016).

[35] U. Chabaud, P. E. Emeriau, and F. Grosshans, Witnessing wigner negativity, Quantum **5**, 471 (2021).

[36] A. Kenfack and K. Zyczkowski, Negativity of the Wigner function as an indicator of non-classicality, J. Opt. B: Quantum Semiclassical Opt. **6**, 396 (2004).

[37] F. Albarelli, M. G. Genoni, M. G. A. Paris, and A. Ferraro, Resource theory of quantum non-Gaussianity and Wigner negativity, Phys. Rev. A **98**, 052350 (2018).

[38] R. Takagi and Q. Zhuang, Convex resource theory of non-Gaussianity, Phys. Rev. A **97**, 062337 (2018).

[39] C. Fabre and N. Treps, Modes and states in quantum optics, Rev. Mod. Phys. **92**, 035005 (2020).

[40] F. Dell'Anno, S. De Siena, and F. Illuminati, Multiphoton quantum optics and quantum state engineering, Phys. Rep. **428**, 53 (2006).

[41] I. Straka, L. Lachman, J. Hlousek, M. Mikova, M. Micuda, M. Jezek, and R. Filip, Quantum non-Gaussian multiphoton light, npj Quantum Inf. **4**, 4 (2018).

[42] M. Walschaers, V. Parigi, and N. Treps, Practical framework for conditional non-gaussian quantum state preparation, PRX Quantum **1**, 020305 (2020).

[43] U. Chabaud, G. Roeland, M. Walschaers, F. Grosshans, V. Parigi, D. Markham, and N. Treps, Certification of non-gaussian states with operational measurements, PRX Quantum **2**, 020333 (2021).

[44] M. Bellini and A. Zavatta, Manipulating light states by single-photon addition and subtraction, Prog. Opt. **55**, 41 (2010).

[45] C. Navarrete-Benlloch, R. Garcia-Patron, J. H. Shapiro, and N. J. Cerf, Enhancing quantum entanglement by photon addition and subtraction, Phys. Rev. A **86**, 012328 (2012).

[46] A. Kitagawa, M. Takeoka, M. Sasaki, and A. Chefles, Entanglement evalution of non-Gaussian states generated by photon subtraction from squeezed states, Phys. Rev. A **73**, 042310 (2006).

[47] T. J. Bartley and I. A. Walmsley, Directly comparing entanglement-enhancing non-Gaussian operations, New J. Phys. **17**, 023038 (2015).

[48] Y. Mardani, A. Shafiei, M. Ghadimi, and M. Abdi, Continuous-variable entanglement distillation by cascaded photon replacement, Phys. Rev. A **102**, 012407 (2020).

[49] O. Černotík and J. Fiurasek, Displacement-enhanced continuous-variable entanglement concentration, Phys. Rev. A **86**, 052339 (2012).

[50] C. N. Gagatsos and S. Guha, Efficient representation of Gaussian states for multimode non-Gaussian quantum state engineering via subtraction of arbitrary number of photons, Phys. Rev. A **99**, 053816 (2019).

[51] X. X. Xu, Enhancing quantum entanglement and quantum teleportation for two-mode squeezed vacuum state by local quantum-optical catalysis, Phys. Rev. A **92**, 012318 (2015).

[52] V. Parigi, A. Zavatta, M. S. Kim, and M. Bellini, Probing quantum commutation rules by addition and subtraction of single photons to/from a light field, Science **317**, 1890 (2007).

[53] J. Wenger, R. Tualle-Brouri, and P. Grangier, Non-Gaussian Statistics from Individual Pulses of Squeezed Light, Phys. Rev. Lett. **92**, 153601 (2004).

[54] K. Takase, J.-i Yoshikawa, W. Asavanant, M. Endo, and A. Furusawa, Generation of optical Schrödinger cat states by generalized photon subtraction, Phys. Rev. A **103**, 013710 (2021).

[55] H. Takahashi, J. S. Neergaard-Nielsen, M. Takeuchi, M. Takeoka, K. Hayasaka, A. Furusawa, and M. Sasaki, Entanglement distillation from Gaussian input states, Nat. Photonics **4**, 178 (2010).

[56] A. Ourjoumtsev, A. Dantan, R. Tualle-Brouri, and P. Grangier, Increasing Entanglement between Gaussian States by Coherent Photon Subtraction, Phys. Rev. Lett. **98**, 030502 (2007).

[57] M. Walschaers, C. Fabre, V. Parigi, and N. Treps, Entanglement and Wigner Function Negativity of Multimode Non-Gaussian States, Phys. Rev. Lett. **119**, 183601 (2017).

[58] M. Walschaers, S. Sarkar, V. Parigi, and N. Treps, Tailoring Non-Gaussian Continuous-Variable Graph States, Phys. Rev. Lett. **121**, 220501 (2018).

[59] Y. S. Ra, A. Dufour, M. Walschaers, C. Jacquard, T. Michel, C. Fabre, and N. Treps, Non-Gaussian quantum states of a multimode light field, Nat. Phys. **16**, 144 (2020).

[60] M. Walschaers, C. Fabre, V. Parigi, and N. Treps, Statistical signatures of multimode single-photon-added and -subtracted states of light, Phys. Rev. A **96**, 053835 (2017).

[61] V. Averchenko, C. Jacquard, V. Thiel, C. Fabre, and N. Treps, Multimode theory of single-photon subtraction, New J. Phys. **18**, 083042 (2016).

[62] G. S. Agarwal and K. Tara, Nonclassical properties of states generated by the excitations on a coherent state, Phys. Rev. A **43**, 492 (1991).

[63] J. Fiurášek, Conditional generation of N-photon entangled states of light, Phys. Rev. A **65**, 053818 (2002).

[64] P. Kok, H. Lee, and J. P. Dowling, Creation of large photon-number path entanglement conditioned on photo detection, Phys. Rev. A **65**, 052104 (2002).

[65] S.-Y. Lee and H. Nha, Second-order superposition operations via Hong-Ou-Mandel interference, Phys. Rev. A **85**, 043816 (2012).

[66] R. J. Glauber, Coherent and incoherent states of the radiation field, Phys. Rev. **131**, 2766 (1963).

[67] A. Zavatta, M. D'Angelo, V. Parigi, and M. Bellini, Remote Preparation of Arbitrary Time-Encoded Single-Photon Ebits, Phys. Rev. Lett. **96**, 020502 (2006).

[68] D. V. Sychev, V. A. Novikov, K. K. Pirov, C. Simon, and A. I. Lvovsky, Entanglement of macroscopically distinct states of light, Optica **6**, 1425 (2019).

[69] A. Zavatta, V. Parigi, and M. Bellini, Experimental nonclassicality of single-photon-added thermal light states, Phys. Rev. A **75**, 052106 (2007).

[70] V. Parigi, A. Zavatta, and M. Bellini, Manipulating thermal states by the controlled addition and subtraction of single photons, Laser Phys. Lett. **5**, 246 (2008).

[71] A. Biswas and G. S. Agarwal, Nonclassicality and decoherence of photon-subtracted squeezed states, Phys. Rev. A **75**, 032104 (2007).

[72] Y. Kurochkin, A. S. Prasad and A. I. Lvovsky, Distillation of The Two-Mode Squeezed State, Phys. Rev. Lett. **112**, 070402 (2014).

[73] D. P. DiVincenzo, P. W. Shor, J. A. Smolin, B. M. Terhal, and A. V. Thapliyal, Evidence for bound entangled states with negative partial transpose, Phys. Rev. A **61**, 062312 (2000).

[74] J. Lee, M. S. Kim, Y. J. Park, and S. Lee, Partial teleportation of entanglement in a noisy environment, J. Mod. Opt. **47**, 2151 (2000).

[75] C. Gerry and P. Knight, *Introductory Quantum Optics* (Cambridge University, Cambridge, England, 2005).

[76] E. Wigner, On the quantum correction for thermodynamic equilibrium, Phys. Rev. **40**, 749 (1932).

[77] J. Weinbub and D. K. Ferry, Recent advances in Wigner function approaches, Appl. Phys. Rev. **5**, 041104 (2018).

[78] N. Spagnolo, C. Vitelli, T. De Angelis, F. Sciarrino, and F. De Martini, Wigner-function theory and decoherence of the quantum-injected optical parametric amplifier, Phys. Rev. A **80**, 032318 (2009).

[79] M. G. Genoni, M. L. Palma, T. Tufarelli, S. Olivares, M. S. Kim, and M. G. A. Paris, Detecting quantum non-Gaussianity via the Wigner function, Phys. Rev. A **87**, 062104 (2013).

[80] H. Pashayan, J. J. Wallman, and S. D. Bartlett, Estimating Outcome Probabilities of Quantum Circuits Using Quasiprobabilities, Phys. Rev. Lett. **115**, 070501 (2015).

[81] V. Cimini, M. Barbieri, N. Treps, M. Walschaers, and V. Parigi, Neural Networks for Detecting Multimode Wigner Negativity, Phys. Rev. Lett. **125**, 160504 (2020).

[82] S. H. Liu, D. M. Han, N. Wang, Y. Xiang, F. X. Sun, M. H. Wang, Z. Z. Qin, Q. H. Gong, X. L. Su, and Q. Y. He, Experimental Demonstration of Remotely Creating Wigner Negativity via Quantum Steering, Phys. Rev. Lett. **128**, 200401 (2022).

[83] M. Walschaers, Y. S. Ra, and N. Treps, Mode-dependent-loss model for multimode photon-subtracted states, Phys. Rev. A **100**, 023828 (2019).

[84] G. Roeland, S. Kaali, V. R. Rodriguez, N. Treps, and V. Parigi, Mode-selective single-photon addition to a multimode quantum field, New J. Phys. **24**, 043031 (2022).

[85] D. Barral and J. Linares, Engineering continuous variable and coherent state bell-like states in a reconfigurable photonic chip, IEEE J. Quantum Electron. **53**, 2640223 (2017).

[86] D. Barral, J. Linares, and D. Balado, Engineering continuous and discrete variable quantum vortex states by nonlocal photon subtraction in a reconfigurable photonic chip, J. Opt. Soc. Am. B **33**, 2225 (2016).

[87] R. Nehra, M. Eaton, O. Pfister, and A. Marandi, All-optical quantum state engineering for rotation-symmetric bosonic codes, in *Conference on Lasers and Electro-Optics*, Technical Digest Series (Optica Publishing Group, 2022), paper FF2I.2.